JOURNAL OF MATERIALS SCIENCE **34** (1999) 3967–3975

The deformation response of sol-gel-derived zirconia thin films on 316L stainless steel substrates using a substrate straining test

P. B. KIRK, R. M. PILLIAR
Centre for Biomaterials, University of Toronto, Toronto, Ontario, Canada M5S 3E3

Thin (78 ± 4 nm), well-bonded zirconia films were formed on 316L stainless steel substrates by dip-coating in an alkoxide precursor solution followed by annealing in air to achieve film densification. X-ray diffraction showed the film to be either metastable cubic or tetragonal zirconia. A substrate-straining test was used to investigate the mechanical characteristics of the film and interface; this protocol has been used previously to estimate interfacial shear strength through a shear-lag model. At strain levels of about 1.5%, 15 times the yield strain of the substrate, through-thickness cracking of the film was observed. These cracks were driven by deformation localized at slip bands on the substrate surface and the cracking pattern reflected the slip band pattern of the underlying substrate; the propagation of long cracks transversely to the applied stress, as observed in similar experiments previously, was not seen and consequently the shear-lag model was not applicable. As a qualitative indication of good adhesion, film debonding was not observed even at high strain levels. A non-quantitative model was proposed which examined stress transfer across the film-substrate interface on a microscopic scale, and suggested how film, substrate and interface properties affect competition between transverse and slip-band-induced modes of film cracking. This model was then used to reconcile the observations of this study with the transverse cracking observed by others.

1. Introduction

Surface modifications may be used to improve the wear and corrosion characteristics of metals and to control special surface properties such as the biocompatibility of surgical implants. Sol-gel thin film technology offers the potential for relatively simple and low temperature processing to produce protective ceramic coatings with controlled chemistry and uniformity.

For a thin film coating such as a sol-gel-derived ceramic to remain functional it must stay well adhered throughout whatever loading the substrate may experience while in service. Substrate straining tests have been used to investigate the mechanical behaviour and bonding of thin brittle films which are well adhered to ductile substrate materials, such as metal and ceramic films on polymeric substrates [1–3], ceramic films on metal substrates [4–9], and brittle chromium films on aluminum and steel substrates [10]. Since strain in the substrates was transferred into the film through the interface, these studies yielded information about the interfaces [1]. Commonly, cracks were observed to form transversely to the applied strain and the transverse crack density was related to shear load transfer properties of the interface by shear-lag models. At high strain levels, these analyses predicted that the crack density would tend to a steady-state value. An interfacial shear strength τ_{max} could then be determined through a force balance on the segments of film separated by transverse cracks; various relationships of the general form

$$\tau_{max} = \frac{\delta \sigma_f}{k\lambda}$$

were developed [1, 4, 5, 11], where λ is a measure of the steady-state crack spacing (either minimum, mean or maximum spacing), δ is the film thickness, σ_f is the tensile fracture strength of the coating, and k is a dimensionless constant of the order of 1.

Zirconia films produced through the sol-gel process have been reported as effective in retarding corrosion of stainless steel in salt and sulphuric acid solutions [12–16], as well as in reducing high temperature oxidation of stainless steel [12, 17, 18] and nickel [19]. Earlier work by our group has been undertaken in order to evaluate sol-gel-derived zirconia as a potential coating for dental and orthopaedic implant applications, and has demonstrated good adhesion of the films to Ti-6Al-4V [9]. In this article we report on the characterization of sol-gel-derived zirconia films deposited on 316L stainless steel, another common medical implant alloy. This system was of interest also in the evaluation of the substrate straining protocol and shear-lag analysis as measures of adhesion and interface behaviour.

2. Experimental

2.1. Substrate preparation and film deposition

Substrates were machined from stainless steel (316L) bar stock to a geometry based on the ASTM E-8 standard for subsize rectangular tensile test specimens. These were polished on one face to a bright mirror finish using an automated polishing machine. The substrates were degreased with acetone and washed in detergent then copious distilled water, and then passivated with 28% nitric acid for one hour, a procedure compliant with ASTM F-86. The passivated substrates were stored under anhydrous alcohol until immediately prior to coating.

Zirconia films were deposited by dip-coating from a precursor solution containing zirconium propoxide in *n*-propanol, with water as catalyst, acetic acid as a chelating agent to control polymerization rates, and ethylene glycol as a plasticizer. Dip-coating was performed within a class 100 laminar flow clean hood in order to reduce air-borne particulate contamination of the films. The coatings were densified by sintering in air: samples were heated in a muffle furnace at 5 °C/min from room temperature to 475 °C, then at 1 °C/min to 500 °C, held at 500 °C for one hour, and furnace cooled. The precursor and coating procedure have been described in detail elsewhere [21].

2.2. Zirconia film characterization

X-ray diffraction (XRD; Siemens D-5000 with CuK_α X-ray source) was performed to examine the crystal structure of the film. Scans were made over the range $2\theta = 25^\circ$ to 65° in increments of 0.02°. Although high order reflections have been recommended for distinguishing between the cubic and tetragonal phases of zirconia [20], no higher angle reflections were detected above background noise levels.

Film thickness was determined by automated ellipsometry (AutoEL-II, Rudolph Research, Flanders NJ) using a signal wavelength of 6328 Å. Thickness values were calculated from Δ and Ψ parameters by software (FILM85, v.3.0, Rudolph Research) running on a desktop computer. The work of Filiaggi *et al.* [21] showed that an assumed value of $n = 1.90$ for the refractive index of these sol-gel-derived zirconia films was acceptable insofar as it gave calculated film thicknesses that agreed with values measured by the stylus technique.

2.3. Substrate straining test

The mechanical behaviour of the zirconia thin film and the zirconia-metal interface were investigated through a substrate straining test. In this test, used previously by Filiaggi *et al.* [9] and based on work by Agrawal and Raj [4, 5], cracks in the thin brittle film were induced through application of a uniaxial strain to the ductile substrate material. Cracks were observed to develop transversely to the applied strain, and through a shear-lag analysis the crack spacing was related to load transfer properties of the interface.

Zirconia-coated tensile test specimens were prepared as described above. Tensile deformation was applied to the samples by a servohydraulic mechanical testing machine (Instron 8501), which was operated under strain control using an extensometer (Instron model 2620-830) to monitor strain levels. This deformation was interrupted at pre-defined strain levels, and the samples were unloaded and examined using SEM for cracks in the zirconia film.

Accompanying this investigation of the cracking behaviour of zirconia-coated substrates was characterization of the strain response of the substrates themselves. The same sequence of incremental straining and SEM observation was performed on uncoated samples which had been polished and passivated by the same procedures as the coated samples. These uncoated samples were also given a heat treatment similar to that used for annealing the sol-gel films (5 °C/min up to 490 °C, 1 °C/min to 500 °C, and hold at 500 °C for one hour before furnace cooling). In order to prevent oxide growth on these uncoated samples the heat treatment was performed in vacuo.

3. Results

Numerous pits were observed in the 316L substrate after polishing, often elongated in the rolling direction of the bar stock. These were attributed to inclusions in the steel which had been pulled out during the polishing procedure. The pits were not generally covered over by the zirconia film, and often acted as nuclei for drying cracks. However, these drying cracks were not observed to propagate far from the pits. The low density of these defects and their lack of interaction with strain-induced modes of cracking in the film after annealing allowed the substrate straining test to be unaffected by their presence. The coatings were free of other gross defects, except for cracking found at geometric discontinuities such as sample edges. Automated ellipsometry measurements indicated that the mean thickness of the zirconia film was 78 nm, with a standard deviation of 4 nm.

The X-ray diffraction spectrum of sol-gel-derived zirconia on 316L stainless steel is shown in Fig. 1, along with that of sol-gel-derived zirconia deposited on Ti-6Al-4V from earlier work [22]. The zirconia/316L spectrum showed only one peak due to zirconia, the strong (*111*) reflection at $2\theta = 30.3^\circ$ characteristic of cubic and/or tetragonal zirconia. The higher order reflections which had been observed in the zirconia/Ti-6Al-4V system were not observed, although the (*220*) reflection at $2\theta \approx 51^\circ$ may have been masked by the 316L substrate signal. The (*111*) reflection was shifted to a slightly lower value of 2θ in the zirconia/316L spectrum than in the zirconia/Ti-6Al-4V spectrum, which was more indicative of tetragonal than cubic zirconia. The disappearance of higher order peaks suggested a smaller crystal size in the zirconia/316L system.

Figs 2–4 show the progressive development of cracks in the zirconia films with increasing substrate strain levels, along with the surface morphology of the polished,

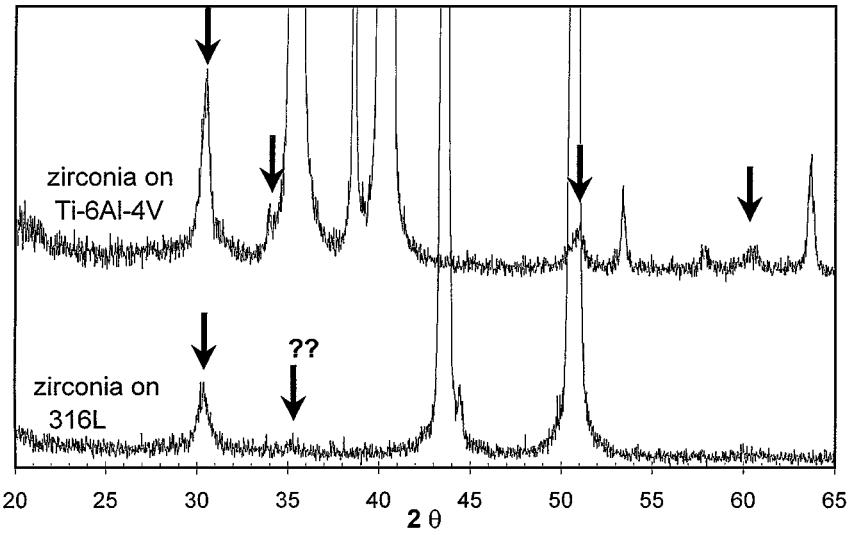

2θ,°	d, Å	Identification
Zirconia on 316L substrate:		
30.3	2.92	c/t ZrO_2 *(111)*
~35.2	~2.55	c/t ZrO_2 *(200)*
43.6	2.08	γ-Fe *(111)*
44.4	2.04	δ-Fe *(110)*
50.7	1.80	γ-Fe *(200)*
Zirconia on Ti-6Al-4V substrate:		
30.5	2.93	c/t ZrO_2 *(111)*
34.0	2.64	c/t ZrO_2 *(200)*
50.8	1.80	c/t ZrO_2 *(220)*
60.4	1.53	c/t ZrO_2 *(311)*

c/t ZrO_2 = cubic or tetragonal zirconia
γ-Fe = austenite, 316L stainless steel
δ-Fe = retained δ-ferrite, 316L stainless steel

Figure 1 X-ray diffraction spectrum of sol-gel-derived zirconia on 316L stainless steel substrate (lower spectrum), and that of zirconia on Ti-6Al-4V. Unmarked peaks are attributed to the substrates; those marked with an arrow are characteristic of cubic and/or tetragonal zirconia. The location marked with "??" may be the (*200*) diffraction signal.

uncoated substrate at equivalent strains. At strains of about 1% a slip band structure was easily observed at the surface of the uncoated samples, and was well developed in those grains with their crystal axes favourably aligned with respect to the tensile axis (note that the yield strain of the mill-annealed 316L substrate was about 0.1%). However, at this strain level cracks were not observed in the zirconia-coated samples. Slip bands were on occasion observed beneath the film without evidence of film fracture, implying some degree of plasticity in the coating.

At higher strains of about 1.5%, localized film cracking was observed in the zirconia-coated samples. The crack pattern which developed was clearly similar to slip band patterns on uncoated steel surfaces. The cracks were short, limited in extent to single grains in the substrate, and did not propagate catastrophically across any great length of the film. The cracks were not oriented transversely to the applied strain; rather they existed in localized groups of parallel cracks with many orientations.

At high strains the crack patterns in the zirconia film continued to be a reflection of the slip band structure in the substrate. Dense slip bands were observed in all grains at the substrate surface; multiple slip systems were active in many grains. At low magnifications (1000×), the coated and uncoated samples were indistinguishable (see Fig. 4, left); at higher magnifications the structure of cracks in zirconia over the slip bands became visible (see Fig. 4, right, and Fig. 5). No delamination of the zirconia film was observed, even on one sample subjected to 23% strain.

4. Discussion

The slip-band-induced cracking observed in this study and in an examination of sol-gel-derived zirconia films on Ti-6Al-4V (results reported elsewhere [22]) is in contrast to observations of transverse cracking by researchers studying materials combinations ranging from the similar (e.g. sol-gel-derived silica films on nickel [5]) to the seemingly identical (sol-gel-derived zirconia films on Ti-6Al-4V [9]). The shear-lag models used previously do not effectively address the phenomena observed in this study of the zirconia/Ti-6Al-4V and zirconia/316L systems. In the shear-lag models a uniform tensile strain is assumed to build up in the film by shear stresses transferred across the interface, and long transverse cracks are observed. However, at the microscopic level the strain in the 316L and Ti-6Al-4V substrates at the interface was not uniform nor was it necessarily parallel to the applied macroscopic stress. Substrate plastic deformation was localized in bands of very high shear strain (slip bands), not as a uniform tensile strain as assumed in the shear-lag model. α-Ti has a hexagonal crystal structure with anisotropic elastic moduli, and therefore even the elastic strain was not necessarily uniform in magnitude or direction. In addition, the strain at slip bands was not confined to the original plane of the surface; out-of-plane displacement across the slip band may also have occurred. None of these factors are addressed in the shear-lag model.

The shear-lag model can only be effective in a case where the stress that builds up in the film is uniform in magnitude (prior to initial film cracking) and direction, and is in the plane of the film. In that case, assuming adequate resistance to debonding, at some critical stress level the film will fail by propagation of cracks from surface, internal, or interfacial flaws and these cracks will propagate in a direction that maximizes the release of strain energy from within the film while minimizing the created surface area. Thus, catastrophic propagation of cracks should occur normal to the stress in the film. This transverse cracking mode of film failure has been observed in brittle films deposited on metal substrates in studies reported by others [4, 5, 7, 10, 21]. Given that the plastic deformation of metals occurs by shear along slip planes, it seems remarkable that any of these

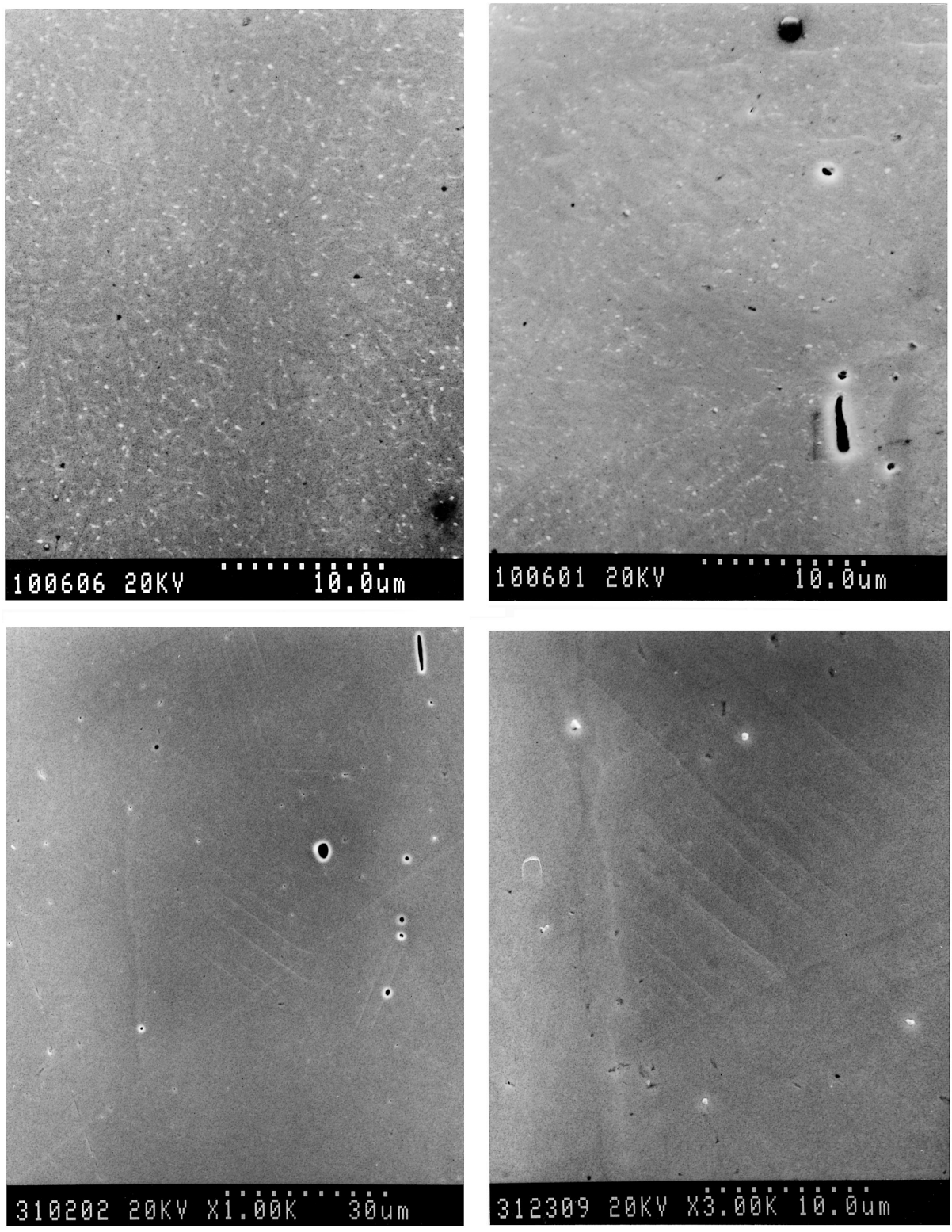

Figure 2 Scanning electron micrographs showing low-strain surface morphology of (top) zirconia-coated 316L stainless steel; and (bottom) uncoated 316L stainless steel. Substrate strain levels: 1.0–1.3%. Note that micrograph at bottom left is at 1000× original magnification; the others are 3000×.

researchers would have observed transverse cracking, especially as the strain levels reported for initial film fracture were in all cases well above substrate yield strains. Agrawal and Raj [4, 5] did report observation of slip bands in the copper and nickel substrates beneath the silica films that they were investigating, but these did not seem to have any effect on film cracking. All cracks observed in their silica films formed normal to the tensile axis irrespective of the orientations and grain boundaries of the underlying substrate grains. Judging from the micrographs which accompanied their article, shear bands were only observed at 25% strain; they were not apparent at 5 and 10% strain, while the transverse crack pattern had almost reached steady state spacing by 10% strain. Agrawal and Raj proposed that slip had not played a role in the initiation of cracks; the crack pattern developed before slip bands became well defined at the surface. Other researchers using a shear-lag

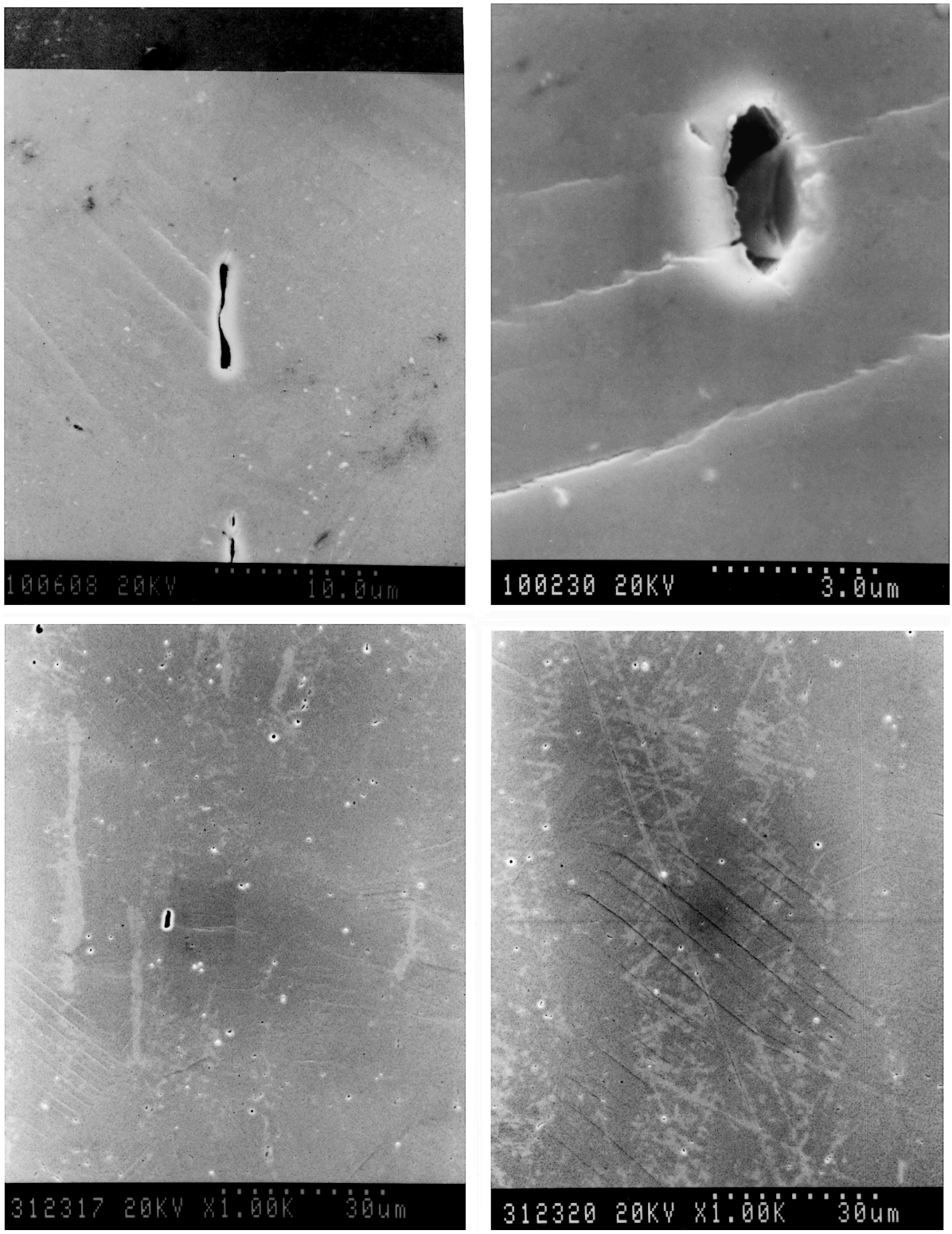

Figure 3 Scanning electron micrographs showing moderate-strain surface morphology of (top) zirconia-coated 316L stainless steel; and (bottom) uncoated 316L stainless steel. Substrate strain levels: 1.5–1.75%.

model to investigate films on metal substrates did not report any observation of slip bands [6–10]. However, Quinson *et al*. [14] in their study of sol-gel-derived zirconia coatings on 304 stainless steel observed slip bands beneath the coating after 5 and 20% strains. The slip bands were observed to cause cracking of thick multi-layer (150 nm thick) coatings, while thin (34 nm) coatings were uncracked after 20% substrate strain.

A simple model is illustrated in Fig. 6 for explaining the observation of transverse cracking in some films and slip-band-induced cracking in others, both deposited on metals which deform primarily by shear along slip planes. In the first case (Fig. 6a), the interface between the film and metal is assumed to be "sharp" and "strong." By a "sharp" interface, it is meant that the surface of the substrate behaves in a manner representative of and dictated by the bulk, i.e. slip lines extend fully to the surface. In assuming a "strong" interface, all strains are transferred from the substrate to the film, and modes such as adhesive failure (debonding) are ignored. In this

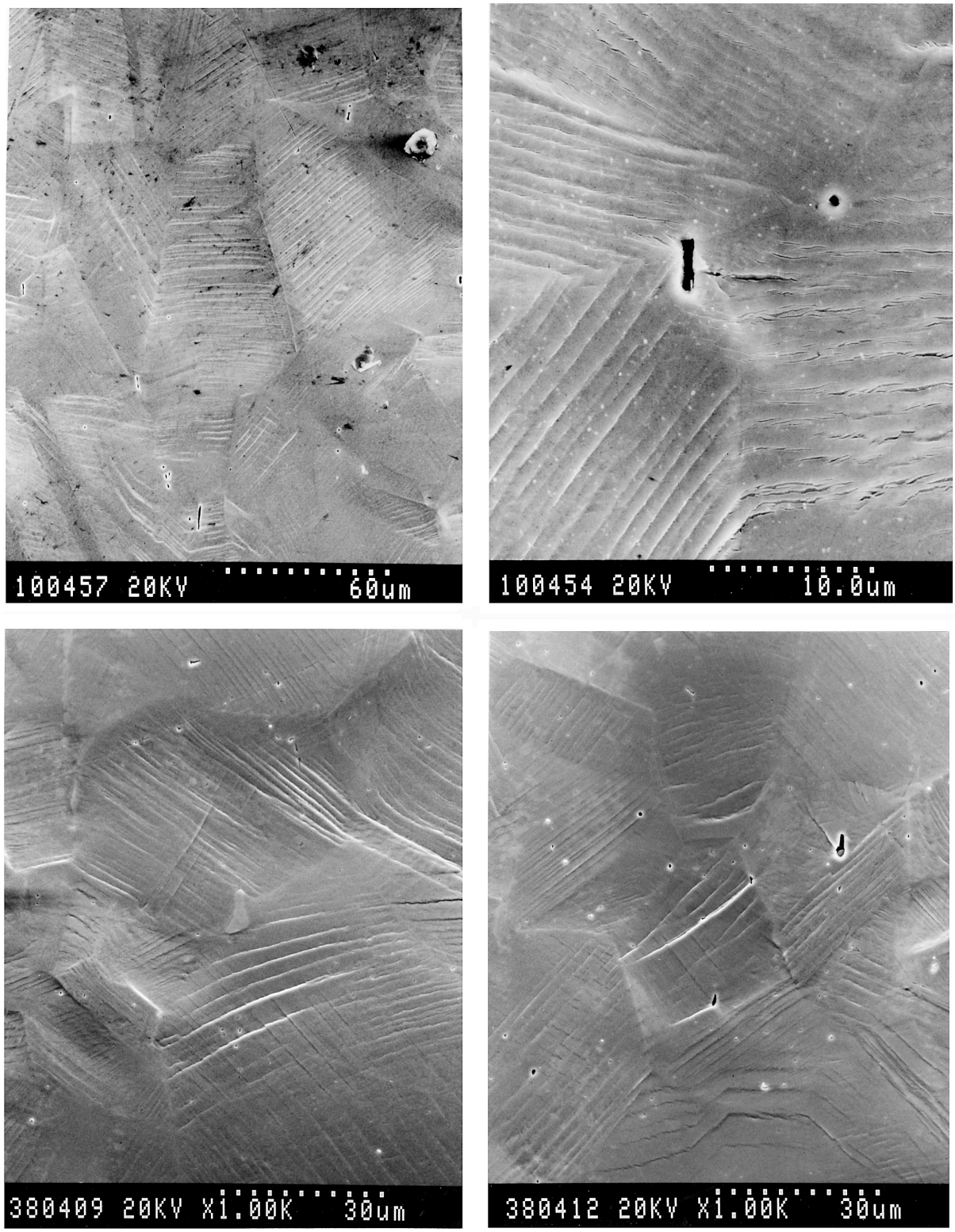

Figure 4 Scanning electron micrographs showing high-strain surface morphology of (top) zirconia-coated 316L stainless steel; and (bottom) uncoated 316L stainless steel. Substrate strain levels: 8%.

case, the strain applied to the interface by substrate deformation is localized at slip bands. These strain concentrations induce stress concentrations in the film which initiate and propagate through-thickness cracks; these are observed as "slip band" cracking patterns in the film. The second case (Fig. 6b) considers an interface that is not "sharp" and "strong" in the sense described above. The surface of the polished metal may be covered by a layer of deformed material which acts to blunt slip bands as they impinge on the surface; recall that slip bands are not observed on poorly prepared surfaces. "Interfacial sliding," i.e. some form of very localized deformation near the interface, may also occur; indeed, this is incorporated into the shear-lag model in the assumption of an interfacial shear strength τ_y. This too would act to delocalize the stress transferred

Figure 5 Electron micrograph of cracks in zirconia film above slip band region of 316L stainless steel.

into the film from slip band strain concentrations in the substrate. If these factors acted sufficiently to diffuse the microscopic strain concentrations in the substrate, the stress and strain transferred to the film would be representative of the macroscopic applied strain, i.e. tensile in nature. Transverse cracking would then be expected, and shear-lag analysis could be applied.

In reality, what probably occurs is somewhere in between these two extremes and is dependent on a number of factors, including:

- *the nature of slip bands in the metal substrate*: How does the slip band structure develop with applied strain? Is strain highly localized in a few very fine slip bands, or more widely dispersed in a greater density of broad, diffuse slip bands?
- *the quality of the metal surface*: How thick is the deformed surface layer, or Beilby zone? How are its mechanical properties and microstructure different from the bulk of the substrate? How does this affect the distribution of strain at the substrate-film interface?
- *the nature of the substrate-film interface zone*: How effectively is stress transferred across the interface? Is some form of "interfacial sliding" possible? How much resistance to debonding exists?
- *the tensile failure strain of the film* ε_f. How much tensile strain must be applied to the film before transverse cracks are initiated?
- *the resistance of the film to bending or shear deformation*: Will the stresses concentrated at slip bands cause the film to crack? Can some plastic deformation be accommodated by the film? If the film is very stiff, it may act to inhibit deformation of the interface and metal surface, thereby diffusing slip bands.

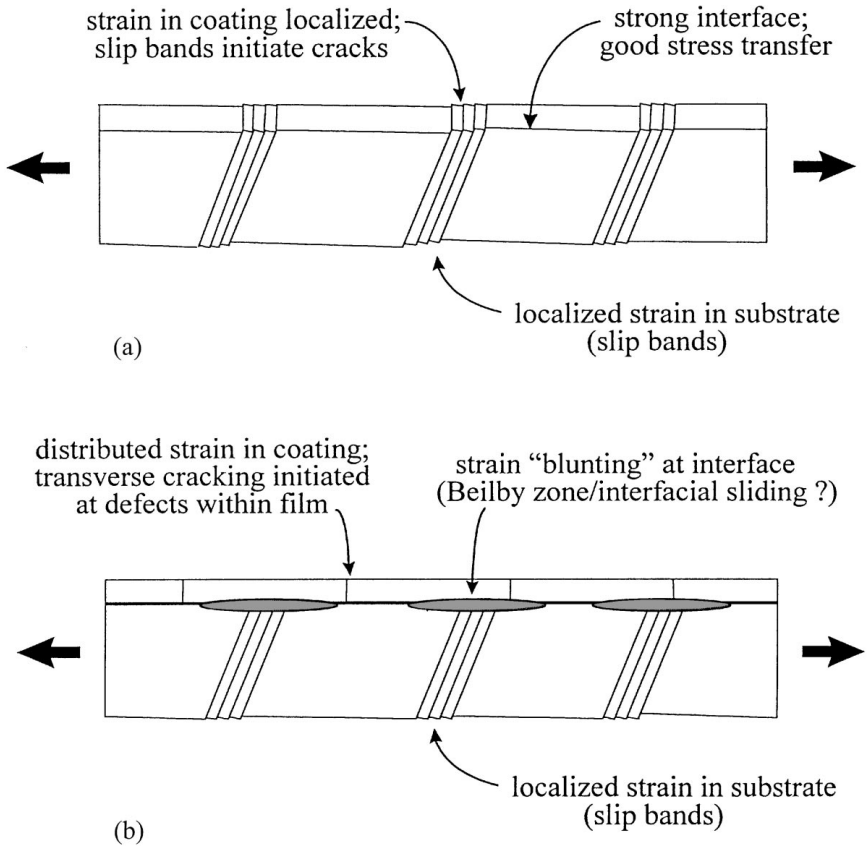

Figure 6 (a) Strain localized at slip bands in the deformed substrate is transferred across an ideal "sharp" interface; localized stress in the coating drives cracks at the slip bands. (b) Strain localized at slip bands in the deformed substrate is diffused by a surface layer of deformed material (e.g. Beilby zone) and sliding at the interface; uniform, delocalized tensile strain in the coating drives propagation of long transverse cracks.

In general, strain in the sub-surface metal is localized in slip bands; as they approach the interface these strain concentrations may be dispersed to some degree by interaction with a surface layer of deformed metal. "Interfacial sliding" may further delocalize the stress transferred across the interface into the film. Consider the stress and strain transferred into the film as divided into two components: shear and bending components localized at slip bands; and a component resulting from the diffused part of the slip band strains. As a simplifying assumption, if this diffused part of the strain is adequately dispersed it may be considered tensile in nature.* If the strain component γ_{sb} (localized at slip bands) exceeds the shear or bending failure strain of the film γ_f then the cracking occurs along slip band lines; if the uniform tensile component ε_{un} of strain in the film exceeds the tensile failure strain of the film ε_f then transverse cracks propagate. The distribution of total strain into these components then controls which failure mode is observed. γ_{sb} and ϵ_{un} are affected by the applied strain, the substrate material, the metal surface condition, the stiffness of the film, and the nature of the interface. γ_f and ϵ_f are materials properties dependent on the film composition and microstructure (porosity, defect size and distribution, etc.).

This model suggests reasons why a previous study using the sol-gel-derived zirconia-Ti-6Al-4V system [9] observed transverse cracking while Kirk *et al*. [22] did not. Two small changes were made to sample preparation protocols for the second study: after machining, the titanium alloy substrates were given a stress-relieving heat treatment; and dip-coating was performed in a near dust-free environment. The heat-treatment, and the possibility of incremental improvement in the quality of polished surfaces, may have produced substrates with a thinner Beilby layer, and therefore sharper slip bands would have been formed at the surface. The reduction in dust-formed defects in the zirconia film could have increased its failure strain. Both of these factors would have tended to promote slip-band-induced cracking over transverse cracking.

While transverse crack patterns are reflective of film and interface properties, the slip-band-induced cracking observed in zirconia films on 316L stainless steel and Ti-6Al-4V produced patterns which were characteristic of the substrate. The properties of the film and interface affected the type of cracking which occurs (i.e. slip-band, not transverse), but had very little effect on the distribution of the slip-band-induced cracks. The patterns were dependent on substrate parameters such as slip band density, grain size, etc., and so no quantitative information regarding film adhesion could be gained by their analysis. The substrate-straining test and shear-lag analysis cannot a priori be assumed to be useful in quantitatively assessing interface strength. Qualitatively, however, the observed behaviour seemed to indicate that adhesion and tensile strength of the zirconia coating were not poor, as no delamination was observed at high strains, and film cracking was not observed until 15 times the 316L substrate yield strain, or 1.5 times that of Ti-6Al-4V.

A preliminary TEM study into the microstructure of sol-gel-derived zirconia showed the film to be well crystallized and composed of 50–100 nm clusters of ~5 nm subgrains, where the orientation of subgrains within each cluster varied by only a few degrees [23]. This nanocrystalline structure was expected to be responsible for the high strain levels accommodated by the film before cracking.

* As an example, consider the case of a system without a 'sharp' and 'strong' interface, as discussed above. The localized shear component is zero and the net sum of the highly dispersed shear strains is equal to the applied macroscopic tensile strain. This is analogous to the relationship between the macroscopic plastic strain observed by deforming a metal in tension and the actual microscopic deformation of grains by shear and grain rotation; the sum (or delocalized average) of the microscopic shear strains and rotations is a macroscopic tensile strain.

Acknowledgements

Funding for this research from the Natural Sciences and Engineering Research Council of Canada is gratefully acknowledged. The authors also wish to thank Dr. Srebri Petrov (Department of Chemistry), for X-ray diffraction analysis; Dr. U. Krull (Department of Chemistry), for use of the automated ellipsometer; and Mrs. Raisa Yakubovich for sol preparation.

References

1. P. H. WOJCIECHOWSKI and M. S. MENDOLIA, *Physics of Thin Films* **16** (1992) 271.
2. Q. GUO, H. OSAKI and L. M. KEER, *J. Appl. Phys.* **68** (1990) 1649.
3. PH. DUCHATELARD, G. BAUD, J. P. BESSE and M. JACQUET, *Thin Solid Films* **250** (1994) 142.
4. D. C. AGRAWAL and R. RAJ, *Acta Metall.* **37** (1989) 1265.
5. *Idem., Mater. Sci. Eng.* **A126** (1990) 125.
6. L. CHANDRA, M. ALLEN, R. BUTTER, N. RUSHTON, A. H. LETTINGTON and T. W. CLYNE, *J. Mater. Sci.: Materials in Medicine* **6** (1995) 581.
7. L. CHANDRA and T. W. CLYNE, *Diamond and Related Materials* **3** (1994) 791.
8. P. M. RAMSEY, H. W. CHANDLER and T. F. PAGE, *Thin Solid Films* **201** (1991) 81.
9. M. J. FILIAGGI, R. M. PILLIAR and D. ABDULLA, *J. Biomed. Mater. Res. (Appl. Biomat.)* **33** (1996) 239.
10. M. S. HU and A. G. EVANS, *Acta Metall.* **37** (1989) 917.
11. R. B. HENSTENBURG and S. L. PHOENIX, *Polymer Composites* **10** (1989) 389.
12. M. ATIK and M. A. AEGERTER, *J. Non-Cryst. Solids* **147/148** (1992) 813.
13. C. CHINO, M. CHARBONNIER, A.-M. DE BECDELIEVRE, C. GUIZARD, M. PAUTHE and J.-F. QUINSON, in Eurogel 1991: Proceedings of the Second European Conference on Sol-gel Technology, Saarbrücken, Germany, 1991, edited by S. Vilminot, R. Nass and H. Schmidt (North-Holland, Amsterdam, 1992) p. 327.
14. J.-F. QUINSON, C. CHINO, A.-M. DE BECDELIEVRE, C. GUIZARD and M. BRUNEL, *J. Mater. Sci.* **31** (1996) 5179.
15. M. ATIK, P. DE LIMA NETO, L. A. AVACA and M. A. AEGERTER, *Ceram. Int.* **21** (1995) 403.
16. M. ATIK, C. R'KHA, P. DE LIMA NETO, L. A. AVACA, M. A. AEGERTER and J. ZARZYCKI, *J. Mater. Sci. Lett.* **14** (1995) 178.
17. K. IZUMI, M. MURAKAMI, T. DEGUCHI and A. MORITA, *J. Amer. Ceram. Soc.* **72** (1989) 1465.

18. M. ATIK, J. ZARZYCKI and C. R'KHA, *J. Mater. Sci. Lett.* **13** (1994) 266.
19. P. C. INNOCENZI, M. GUGLIELMI, M. GOBBIN and P. COLOMBO, *J. Eur. Ceram. Soc.* **10** (1992) 431.
20. R. SRINIVASAN, R. J. DE ANGELIS, G. ICE and B. H. DAVIS, *J. Mater. Res.* **6** (1991) 1287.
21. M. J. FILIAGGI, R. M. PILLIAR, R. YAKUBOVICH and G. SHAPIRO, *J. Biomed. Mater. Res. (Appl. Biomater.)* **33** (1996) 225.
22. P. B. KIRK, M. J. FILIAGGI, R. N. S. SODHI and R. M. PILLIAR, *J. Biomed. Mater. Res. (Appl. Biomater.)* in press (1999).
23. P. B. KIRK and R. M. PILLIAR, submitted (1998).

Received 5 August 1998
and accepted 10 February 1999